ORIGINAL ARTICLE

*Journal of Cachexia, Sarcopenia and Muscle* (2018)
Published online in Wiley Online Library (wileyonlinelibrary.com) **DOI:** 10.1002/jcsm.12360

# Cachexia induced by cancer and chemotherapy yield distinct perturbations to energy metabolism

Fabrizio Pin[1,2], Rafael Barreto[3], Marion E. Couch[2,4,5,6], Andrea Bonetto[1,2,3,4,5,6*] & Thomas M. O'Connell[2,4,5,6*]

[1]*Department of Anatomy and Cell Biology, Indiana University School of Medicine, Indianapolis, IN 46202, USA,* [2]*Indiana Center for Musculoskeletal Health, Indiana University School of Medicine, Indianapolis, IN 46202, USA,* [3]*Department of Surgery, Indiana University School of Medicine, Indianapolis, IN 46202, USA,* [4]*Department of Otolaryngology–Head & Neck Surgery, Indiana University School of Medicine, Indianapolis, IN 46202, USA,* [5]*Simon Cancer Center, Indiana University School of Medicine, Indianapolis, IN 46202, USA,* [6]*IUPUI Center for Cachexia Research, Innovation and Therapy, Indiana University School of Medicine, Indianapolis, IN 46202, USA*

## Abstract

**Background** Cancer cachexia is a metabolic disorder involving perturbed energy balance and altered mitochondrial function. Chemotherapy is a primary treatment option for many types of cancer, but there is substantial evidence that some chemotherapeutic agents can also lead to the development and progression of cachexia. In this study, we apply a comprehensive and systems level metabolomics approach to characterize the metabolic perturbations in murine models of cancer-induced and chemotherapy-induced cachexia. Knowledge of the unique pathways through which cancer and chemotherapy drive cachexia is necessary in order to develop effective treatments.

**Methods** The murine Colon26 (C26) adenocarcinoma xenograft model was used to study the metabolic derangements associated with cancer-induced cachexia. *In vivo* administration of Folfiri (5-fluorouracil, irinotecan, and leucovorin) was used to model chemotherapy-induced cachexia. Comprehensive metabolic profiling was carried out using both nuclear magnetic resonance-based and mass spectrometry-based platforms. Analyses included plasma, muscle, and liver tissue to provide a systems level profiling.

**Results** The study involved four groups of CD2F1 male mice ($n$ = 4–5), including vehicle treated (V), C26 tumour hosts (CC), Folfiri treated (F), and C26 tumour hosts treated with Folfiri (CCF). Significant weight loss including skeletal muscle was observed for each of the experimental groups with the tumour hosts showing the most dramatic change (−3.74 g vs. initial body weight in the CC group). Skeletal muscle loss was evident in all experimental groups compared with V, with the CCF combination resulting in the most severe depletion of quadriceps mass (−38% vs. V; $P < 0.001$). All experimental groups were characterized by an increased systemic glucose demand as evidenced by decreased levels of circulating glucose (−47% in CC vs. V; $P < 0.001$) and depletion of liver glucose (−51% in CC vs. V; $P < 0.001$) and glycogen (−74% in CC vs. V; $P < 0.001$). The cancer-induced and chemotherapy-induced cachexia models displayed unique alterations in flux through the tricarboxylic acid cycle and β-oxidation pathways. Cancer-induced cachexia was uniquely characterized by a dramatic elevation in low-density lipoprotein particles (+6.9-fold vs. V; $P < 0.001$) and a significant increase in the inflammatory marker, GlycA (+33% vs. V; $P < 0.001$).

**Conclusions** The results of this study demonstrated for the first time that cancer-induced and chemotherapy-induced cachexia is characterized by a number of distinct metabolic derangements. Effective therapeutic interventions for cancer-induced and chemotherapy-induced cachexia must take into account the specific metabolic defects imposed by the pathological or pharmacological drivers of cachexia.

**Keywords** Cachexia; Cancer; Chemotherapy; Metabolomics; Metabolism; Muscle wasting

*Received: 1 March 2018; Accepted: 11 September 2018*
**Correspondence to: Andrea Bonetto, Department of Surgery, Indiana University School of Medicine, Indianapolis, 46202 IN, USA. Email: abonetto@iu.edu*
*Thomas M. O'Connell, Department of Otolaryngology–Head & Neck Surgery, Indiana University School of Medicine, Indianapolis, 46202 IN, USA. Email: thoconnell@iu.edu*

## Introduction

As patients with cancer progress along their disease trajectory, it is common for them to be afflicted by the severe wasting syndrome known as cancer-induced cachexia. In some cancers, the prevalence of cachexia in the advanced stages is nearly 80%, and the consequences of this wasting will be the ultimate cause of mortality in ~30% of patients.[1,2]

Cachexia is distinct from starvation, age-related loss of muscle mass (often referred to as sarcopenia), anorexia, malabsorption, and hyperthyroidism.[3]

There is an increasing recognition that cancer cachexia is a metabolic disorder involving perturbed energy balance and altered mitochondrial function.[4–8] The major drivers of these dysfunctions are an extreme inflammatory response and impaired signalling related to muscle protein turnover.[1] Although cachexia is often accompanied by reduced food intake and anorexia, it is clearly distinct from starvation, and the alterations to energy metabolism cannot be corrected by increased nutritional intake alone.[1]

One of the first lines of treatment for cancer patients is often chemotherapy, but there is increasing evidence that some chemotherapeutic agents actually contribute to the development and progression of cachexia. Studies in healthy rats have demonstrated that chemotherapeutic agents including cyclophosphamide, 5-fluorouracil, cisplatin, and methotrexate induce a negative nitrogen balance and commensurate weight loss.[9] Daumrauer *et al.* reported that cisplatin, CPT-11, adriamycin, and etoposide lead to muscle wasting via activation of NF-κB but are independent of the usual cancer-associated up-regulations in the ubiquitin proteasome system.[10] Studies from our laboratory using the combination therapy Folfiri (5-fluorouracil, leucovorin, and irinotecan) have shown that wasting is dependent upon activation of ERK1/2 and p38 mitogen-activated protein kinases pathways but is independent of the ubiquitin proteasome system.[6] In contrast, another study of cisplatin demonstrated an up-regulation of myostatin and the ubiquitin proteasome system.[11,12] Oxidative stress has also been identified as a consequence of a number of chemotherapeutic agents, which could induce muscle wasting via mitochondrial dysfunction.[5,6,10,13,14] These studies highlight the complexity of the muscle wasting effects of chemotherapy and suggest that more detailed studies are needed to deconvolve the mechanisms that drive both cancer-associated and chemotherapy-induced cachexia.

Given the profound metabolic derangements that accompany cachexia, there has been a surprising paucity of detailed metabolomics investigations in this area. The advantage of a metabolomics approach is that an individual's metabolic state represents the combined influences of age, genetics, diet, environmental exposures, and disease state. As such, it more closely represents the functional phenotype of the individual. In one of the earliest metabolomics studies of cachexia, the mouse Colon26 (C26) adenocarcinoma model demonstrated distinct alterations in glucose and lipid metabolism.[15] A later study using the same murine model clarified that the serum metabolome of cachexia was clearly distinct from the effects of starvation or tumour burden.[16] A more recent metabolomics study in an aggressive cachexia-inducing kidney cancer model found that tumour-secreted factors induce excessive fatty acid oxidation leading to oxidative stress, p38 activation, and impaired muscle growth.[17] To date, there have been no metabolomics investigations into the metabolic pathways involved in chemotherapy-induced cachexia.

In this study, we applied a comprehensive and systems level metabolomics approach to investigate the similarities and differences between cancer-induced and chemotherapy-induced cachexia. Our analytical approach involved three separate platforms selected to provide detailed coverage of the major energetic pathways. The nuclear magnetic resonance (NMR) platform detected a wide range of metabolites including those from glycolysis, the tricarboxylic acid (TCA) cycle, and amino acid metabolism. The targeted mass spectrometry platform was selected to provide details on lipid metabolism. Lastly, an NMR-based lipoprotein analysis was selected to provide details on a range of lipoprotein particle sizes and numbers relating to lipid and cholesterol metabolism. In order to provide a more holistic evaluation of energy metabolism, we analysed not only blood plasma but also muscle and liver tissue. Our study utilizes the well-established C26 colorectal tumour model of cancer cachexia and treatment with Folfiri as a model of chemotherapy-induced cachexia.

## Materials and methods

### *Animals*

All animal experiments were conducted with the approval of the Institutional Animal Care and Use Committee at Indiana University School of Medicine and were in compliance with the National Institutes of Health Guidelines for Use and Care of Laboratory Animals and with the ethical standards laid down in the 1964 Declaration of Helsinki and its later amendments. For this study, we used 8-week-old CD2F1 male mice (Harlan, Indianapolis, IN, USA). The animals were maintained on a regular dark–light cycle (light from 8 a.m. to 8 p.m.), with free access to food and water during the whole experimental period. Mice were divided randomly into four groups: mice inoculated with vehicle (V; saline), serving as controls ($n$ = 4) and animals treated with Folfiri (F; $n$ = 5). For the tumour-bearing animals (CC), 10 mice were injected


DOI: 10.1002/jcsm.12360

intrascapularly (s.c.) with $1 \times 10^6$ C26 adenocarcinoma cells in sterile saline, treated or not with Folfiri (CCF).[18] The two groups administered with Folfiri received twice a week combination of 5-fluorouracil (50 mg/kg), leucovorin (90 mg/kg), and CPT-11 (24 mg/kg) intraperitoneal (i.p.) starting at Day 5 after tumour injection (all drugs were purchased from Sigma-Aldrich, St. Louis, MO, USA). Based on previous findings, the amount of drugs delivered to the animals was not exceeding clinically relevant concentrations.[6] Animals were monitored and weighed daily until the day of sacrifice. The animals were sacrificed when body weight loss was at least 10% compared with the initial body weight (a condition referred to as 'moderate cachexia' based on Evans *et al*.[3]), also in line with our previously published findings.[19] At time of sacrifice, no animals were excluded from the study. Several tissues were collected, weighed, snap frozen in liquid nitrogen, and stored at −80°C for further studies. The tibialis anterior muscle was frozen in liquid nitrogen-cooled isopentane, mounted in Optimal Cutting Temperature medium, and stored for morphological analyses. Total blood was withdrawn from anaesthetized mice by cardiac puncture and collected in heparinized tubes. To separate plasma from the haematocrit, all the blood was centrifuged in a haematocrit centrifuge for 15 min at 3500 rpm.

## Cell lines

Murine C26 cells were provided by Donna McCarthy (Ohio State University) and cultured in high glucose (4.5 g/L) Dulbecco's modified Eagle's medium supplied with 10% foetal bovine serum, 1% glutamine, 1% sodium pyruvate, and 1% penicillin/streptomycin. Cells were maintained in a 5% $CO_2$, 37°C humidified incubator.

## Muscle grip strength

The evaluation of the whole body strength in mice was assessed as described in Bonetto *et al*.[20] A forelimb grip strength blinded test was performed at Day 14 after tumour implantation by using a commercial digital grip strength dynamometer (Columbus Instruments, Columbus, OH, USA). Overall, five measurements were completed, and only the top three measurements (peak force, expressed in grams) were included in the analysis.[20]

## Muscle cross-sectional area

Ten-micrometre-thick cryosections of tibialis anterior muscles taken at the mid-belly were incubated overnight with polyclonal anti-laminin (1:1000; Sigma-Aldrich) to label the basement membranes of the muscle cells.[20] Sections were then incubated for 1 h with Alexa Fluor 594-conjugated secondary goat anti-rabbit IgG (Invitrogen, Carlsbad, CA, USA). All samples were observed under an Axio Observer.Z1 motorized microscope (Zeiss, Oberchoken, Germany), and images were recorded for morphometric examination. For determination of the cross-sectional area, muscle fibre size ($n$ = 300–500 per sample) was measured by using the ImageJ 1.43 software.

## Quantification of LDL receptor in liver and skeletal muscle homogenates

The levels of LDL receptor were measured in liver and skeletal muscle homogenates from all groups by using a specific ELISA kit (#MLDLR0; Bio-Techne Corporation, Minneapolis, MN, USA), according to the manufacturers protocol.

## Enzymatic activity

The enzymatic activities of hexokinase, pyruvate dehydrogenase (PDH), citrate synthase (CS), and succinate dehydrogenase (SDH) were measured using Colorimetric Assay Kits (#MAK091, MAK183, #CS0720, #MAK051, and #MAK197, respectively) from Sigma-Aldrich according to the manufacturer's instruction. Briefly, 10 mg of skeletal muscle tissue was homogenized in 100 μL of ice-cold assay buffer and then centrifuged, and 10 μL of homogenate was added to 96-well plates. Appropriate reaction mix was added to each of the wells and the product of enzyme reaction, which results in a colorimetric (600 nm for SDH, 450 nm for hexokinase, Acon, and PDH, and 412 nm for CS) product proportional to the enzymatic activity. The absorbance was recorded by incubating the plate at 37°C taking measurements (600, 450, or 412 nm) every 5 for 30 min.

## Sample preparation for nuclear magnetic resonance

Plasma samples for NMR analysis were prepared diluting 100 μL of plasma with 500 μL of a deuterated phosphate buffer solution (pH = 7.4) containing 2,2,-dimethyl-2-silapentane-5-sulfonate sodium salt (DSS) with a final concentration of 0.5 mM to be used as a chemical shift and quantitation reference. The solution was then filtered through a 10 KDa molecular weight cut-off filter to remove the proteins. Samples were placed in 5 mm NMR tube for analysis. Muscle and liver tissues for NMR analysis were prepared according to the methanol/chloroform water procedure described by Beckonert *et al*.[21] (Nature Protocols, 2, 2692, 2007). Tissue samples of ~100 mg were used for all sample, but actual weights were recorded to normalize the data.


DOI: 10.1002/jcsm.12360

### *Sample preparation for mass spectrometry*

Samples for targeted mass spectrometry analysis were conducted using the Biocrates AbsoluteIDQ kit (Biocrates, Innsbruck, Austria). Each plate contains 16 wells reserved for selected internal standards to optimize the metabolite quantification. For serum analysis, 10 μL aliquots were loaded directly into the 96-well plate followed by derivatization and extraction per vendor protocols. Muscle and liver tissue were prepared according to vendor protocols (Biocrates, *Preparation of Tissue and Feces Samples for Metabolic Phenotyping*, version 1.0).

### *Nuclear magnetic resonance data collection*

Nuclear magnetic resonance data were acquired on a Bruker Avance III 700 MHz NMR spectrometer with a TXI triple resonance probe operating at 25°C. Spectra were collected with a 1D NOESY pulse sequence covering 12 ppm. The spectra were digitized with 32 768 points during a 3.9 s acquisition time. The mixing time was set to 100 ms, and the relaxation delay between scans was set to 2.0 s.

### *Nuclear magnetic resonance lipoprotein profiling*

Determination of lipoprotein particle subfractions by NMR was assessed using the NMR-based platform at LipoScience (now LabCorp, Morrisville, NC, USA). Lipoprotein particle numbers and sizes were determined using a version of the LP2 algorithm[22] modified for murine plasma. GlycA levels were quantified as described by Otvos *et al*.[23]

### *Nuclear magnetic resonance data processing*

The data were processed using Advanced Chemistry Development Spectrus Processor (version 2016.1; Toronto, Canada). The spectra were zero filled to 65 536 points and apodized using a 0.3 Hz decaying exponential function and fast Fourier transformed. Automated phase correction and third-order polynomial baseline correction were applied to all samples. Metabolite concentrations were quantified using the Chenomx NMR Suite (version 8.2; Edmonton, Canada). The DSS-$d_6$ was used as a chemical shift and quantification reference for all spectra and was set to a chemical shift of 0.00 and a concentration of 500 μM. Quantitative fitting of each spectrum was carried out in batch mode, followed by manual adjustment for some spectra to correct for errors arising from spectral overlap. For tissue samples, the final concentrations were normalized based on the weight of the tissue used to prepare each sample. The quantification of glycogen in muscle and liver tissue was carried out using spectral integration rather than spectral fitting with the Chenomx software. As glycogen is a heterogeneous polysaccharide of different chain lengths, the NMR signals are composed of overlapping peaks in specific windows of the spectrum. The integration range from 5.37 to 5.43 ppm was used, and the concentrations are given in spectral intensity units.

### *Mass spectrometry data collection*

This Biocrates AbsoluteIDQ p180 assay quantifies 188 metabolites from six chemical classes: acylcarnitines (ACs), amino acids, biogenic amines, hexoses (sum of hexoses), PCs, and sphingomyelins. Data were collected on an AB Sciex 4000 QTRAP coupled to an Acquity UPLC system with the selective mass-spectrometric detection using multiple reaction monitoring pairs. The amino acids and biogenic amines were detected using a liquid chromatography tandem mass spectrometry method, and the lipid species were detected using a flow injection analysis tandem mass spectrometry method per vendor-defined settings.

### *Mass spectrometry data analysis*

Data analysis including normalization (tissue weight) for quantification of metabolite concentrations and quality assessment was performed with the MetIDQ software package, which is an integral part of the AbsoluteIDQ kit. The metabolite concentration of each metabolite in each experimental condition was compared with the measurement detection limit specifications as reported by the manufacturer of the AbsoluteIDQ p180 kit (Biocrates). A metabolite was excluded from further analyses if its concentration measurement data did not meet all of the following criteria: (i) minor of 20% of missing values (non-detectable peak) for each quantified metabolite in each experimental group and (ii) 50% of all measured sample concentrations for the metabolite had to be above the limit of detection.

### *Reactive oxygen species analysis*

Reactive oxygen species (ROS) were detected using the 2,7-dichlorofluorescein diacetate (DCFH-DA) as a probe. Briefly, gastrocnemius muscles were homogenized in 1.5 mL of Milli-Q $H_2O$. Muscle homogenates were then centrifuged 6 min at 13 000 rpm at 4°C and the supernatant collected. For each sample, a 10 μL aliquot was mixed with 10 μL of a 5 μM solution of DCFH-DA. After 15 min of incubation at 37°C, 1 mL of cold reaction buffer (0.1 M $KPO_4$, pH 7.4, 0.1% (*v*/v) Triton X-100) was added to each sample and kept on ice. DCFH-DA fluorescence was detected by using


DOI: 10.1002/jcsm.12360

fluorimeter (488 nm ex/525 nm em). The data expressed as arbitrary unit were normalized for the total protein content.

### Real-time quantitative polymerase chain reaction

RNA from quadriceps was isolated using the miRNeasy Mini Kit (Qiagen, Valencia, CA, USA) and following the protocol provided by the manufacturer. RNA was quantified by using a Synergy H1 spectrophotometer (BioTek, Winooski, VT, USA). RNA integrity was checked by electrophoresis on 1.2% agarose gel containing 0.02 mol/L morpholinopropanesulfonic acid and 18% formaldehyde. Total RNA was reverse transcribed to cDNA by using the Verso cDNA kit (Thermo Fisher Scientific, Waltham, MA, USA). Transcript levels were measured by real-time PCR (Light Cycler 96, Roche, Indianapolis, IN, USA) taking advantage of the TaqMan gene expression assay system (Life Technologies, Carlsbad, CA, USA). In particular, expression levels for phosphoenolpyruvate carboxykinase (PEPCK; Mm00551411_m1) were detected. Gene expression was normalized to TATA-binding protein (Mm01277042_m1) levels using the standard $2^{-\Delta CT}$ methods.

### Statistics

Statistical comparison of metabolites for each of the groups was carried out in GraphPad Prism (GraphPad, La Jolla, CA, USA) using a one-way analysis of variance with Tukey's multiple comparison test.

## Results

### Cancer and chemotherapy both induce reductions in skeletal muscle mass and function

The *in vivo* models of cancer-induced and chemotherapy-induced cachexia all demonstrate significant alterations in body composition and function. The four groups in this study will be referred to as vehicle (V), cancer cachexia (CC), Folfiri treated (F), and cancer cachexia treated with Folfiri (CCF). *Figure* 1A shows the body weight changes observed for each of the four groups, while *Figure* 1B shows the absolute changes in body weight in the groups. The F group received the first treatment on Day 5, and after an initial increase in body weight, starting Day 12 they exhibited a slow decline in weight until sacrifice at Day 37, in accordance with our previously published observations.[6] The CC group displayed a rapid and precipitous decline in weight starting near Day 8 until sacrifice at Day 13.[18] The CCF group had a similarly dramatic decline in body weight as the CC group, although their overall survival was improved following the administration of chemotherapy. Because of this, the size of the tumour in the CCF group was significantly larger than in the CC group (*Figure* 1C). Muscle weight was significantly reduced in the CC and F groups, while, consistent with a larger tumour size, it was significantly exacerbated in the CCF group (*Figure* 1D). In a similar manner, adipose tissue was significantly depleted in the CCF animals, while fat loss was more moderate in the CC and F groups (*Figure* 1E). Consistent with a depletion of muscle mass, a reduction in muscle grip strength (*Figure* 1F) and a decrease in muscle fibre cross-sectional areas (40–50% vs. V) in the three experimental groups (*Figure* 1G) were also detected.

### Plasma metabolome indicates difference in cellular energetics with cancer cachexia and chemotherapy

A multiplatform metabolomics approach was conducted to look for differences in the major cellular energy pathways. *Figure* 2 shows several metabolites representative of glycolysis and the TCA cycle. A significant decrease in circulating glucose of nearly 50% was observed in the CC group. A trend of reduced plasma glucose of around 30% was observed for both the F and CCF groups (*P*-values = 0.08 for each group compared with vehicle). These data indicate an overall increase in glucose consumption or alternatively a significant decrease in glucose production. At the end of the glycolytic pathway, the pyruvate levels were not statistically different from V, but the reduction in the CC group came close with a *P*-value = 0.06. The lactate concentrations in each of the experimental groups were not significantly different from V, although the level in the CCF group was significantly higher than in CC. This suggests some degree of drug-induced mitochondrial stress, which would lead to an accumulation of lactate.

The levels of citrate and succinate in the TCA cycle showed dramatic alterations. In the CC group, both of these metabolites were reduced by around 80%, consistent with a decreased flux through the TCA cycle. In contrast, the citrate and succinate levels in the F group were not significantly different from the V group. The reductions in the CCF group were consistent with the CC group suggesting that the cancer-induced cachexia plays a dominant role in TCA cycle flux.

### Differences in branched chain amino acid and fatty acid oxidation in cancer cachexia and chemotherapy

The levels of branched chain amino acids (BCAAs) presented an interesting difference between the CC and F groups (*Figure* 3A). In particular, the levels of isoleucine and valine


DOI: 10.1002/jcsm.12360

**Figure 1** Morphological and functional changes associated with cancer-induced and chemotherapy-induced cachexia. Body weight (BW) curves (A) and BW change (B) in vehicle-treated animals (V), C26 hosts (CC), Folfiri-treated mice (F), or Folfiri-treated tumour bearers (CCF). Tumour size measured at sacrifice in CC and CCF groups (C). Gastrocnemius (GSN), tibialis anterior (TA), and quadriceps (Quad) muscle weights (D). Liver, spleen, and fat weights (E). All tissues and organs were normalized to the initial body weight (IBW) and expressed as weight/100 mg IBW. Whole body forelimb voluntary grasping strength, measured 13 days after tumour inoculation reported as peak force, was measured by taking advantage of a grip strength metre and expressed as the average of the three top pulls from each animal (F). Quantification of the cross-sectional area (CSA) in TA and representative images obtained after immunofluorescence staining of TA muscle cross sections for laminin (red) (G). Data are expressed as means ± standard deviation. Statistical significance was evaluated by two-way analysis of variance, and significant differences (at least $P < 0.05$) were reported as $^{a}P$ vs. V; $^{b}P$ vs. CC; $^{c}P$ vs. F.

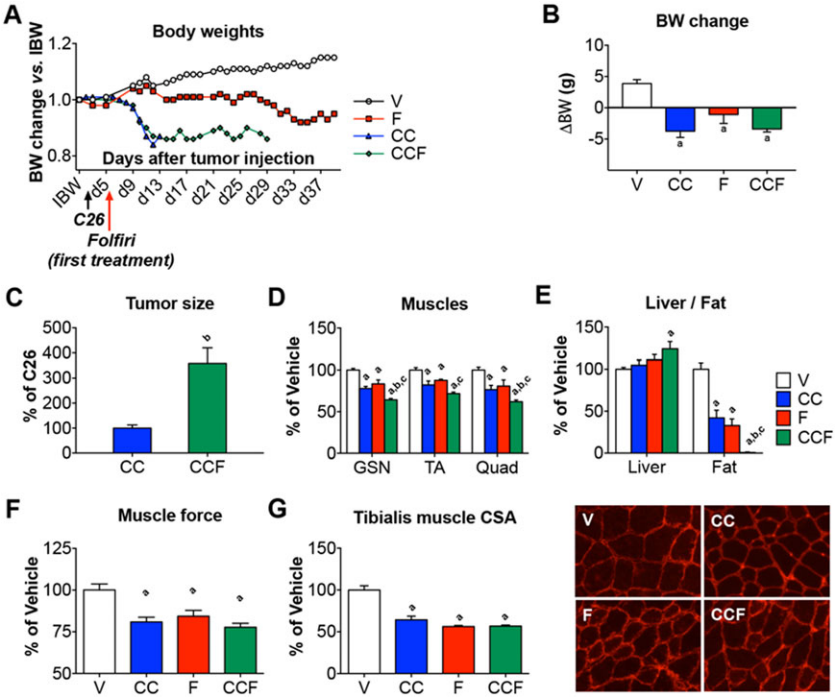


were significantly reduced in the CC group, while for all three BCAAs, the levels were higher in the F group than in the CC animals. This suggests clear differences in the amino acid catabolism and oxidation pathways. In the CCF group, the administration of chemotherapy appears to provide some level of recovery of the BCAA levels to those in the V group.

Acylcarnitines are formed from a family of carnitine acyltransferases that exchange a CoA group for a carnitine. AcylCoA species cannot cross the mitochondrial membrane, but the ACs can. Once inside the mitochondria, these transferases can shuttle the ACs out of the mitochondria into the circulation. Serum ACs are thus a useful metabolic surrogate for intermediates along the β-oxidation pathway. *Figure* 3B shows the three shortest ACs. The C0 species is carnitine with no fatty acid attached. The levels of C0 are expected to increase with the concentration of fatty acids in the blood to facilitate transport into the mitochondria for fatty acid oxidation. The reduced level in the CC group may indicate lower levels of fatty acids in the blood or simply reduced fatty acid entry into the mitochondria. In the F group, the levels were not significantly different from V. The CCF group displayed an intermediate level.

The C2 species is acetylcarnitine, which is in equilibrium with acetyl-CoA. In all three experimental groups, the levels were lower, which would be consistent with reduced acetyl-CoA production, but the reduction was more pronounced in the CC and CCF groups. The C3 species (propionyl carnitine) can be derived from oxidation of fatty acids and BCAAs. The comparatively higher levels of C3 in the F group compared with the CC and CCF groups demonstrated altered flux of fatty acids and/or BCAAs through the β-oxidation pathway. The levels of selected medium and long chain ACs are shown in *Figure* 3C. These data suggest a trend of reduced flux through β-oxidation in both the CC and F groups with the exception of the increased level of the C8 AC in the CCF group.

## *Large changes in lipoprotein metabolism in cancer cachexia*

One of the most striking findings was a dramatic increase in the number of low-density lipoprotein particles (LDL-Ps) in the CC and CCF groups. *Figure* 4A shows that the LDL-


DOI: 10.1002/jcsm.12360

**Figure 2** Glycolysis and tricarboxylic acid (TCA) cycle plasma intermediates are affected by cancer and chemotherapy. Representative diagram of glycolysis and TCA cycle showing the metabolites concentration (expressed in mM) detected in the plasma of vehicle-treated animals (V), C26 hosts (CC), Folfiri-treated mice (F), or Folfiri-treated tumour bearers (CCF). Data are expressed as means ± standard deviation. Statistical significance was evaluated by two-way analysis of variance, and significant differences (at least $P < 0.05$) were reported as $^{a}P$ vs. V; $^{b}P$ vs. CC; $^{c}P$ vs. F.

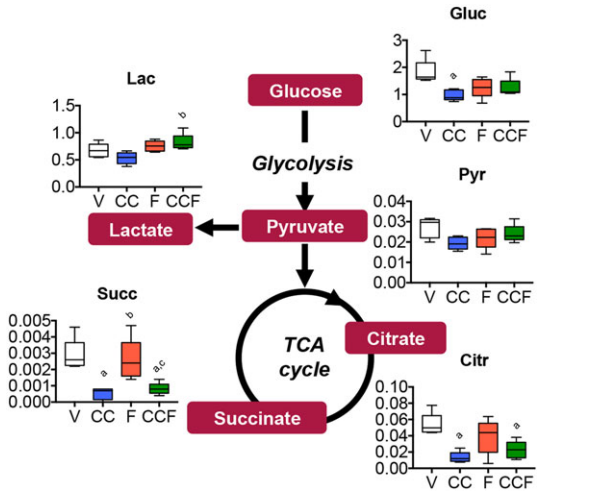


**Figure 3** Plasma metabolites involved in amino acid and fatty acid metabolism. Leucine (Leu), isoleucine (Iie), and valine (Val) levels (expressed in mM) in the plasma of vehicle-treated animals (V), C26 hosts (CC), Folfiri-treated mice (F), or Folfiri-treated tumour bearers (CCF) (A). Free carnitine (C0), acetylcarnitine (C2), acylcarnitine (C3), octanoylcarnitine (C8), decanoylcarnitine (10), and palmitoylcarnitine (16) levels (expressed in mM) in the plasma of vehicle-treated animals (V), C26 hosts (CC), Folfiri-treated mice (F), or Folfiri-treated tumour bearers (CCF) (B). Data are expressed as means ± standard deviation. Statistical significance was evaluated by two-way analysis of variance, and significant differences (at least $P < 0.05$) were reported as $^{a}P$ vs. V; $^{b}P$ vs. CC; $^{c}P$ vs. F.

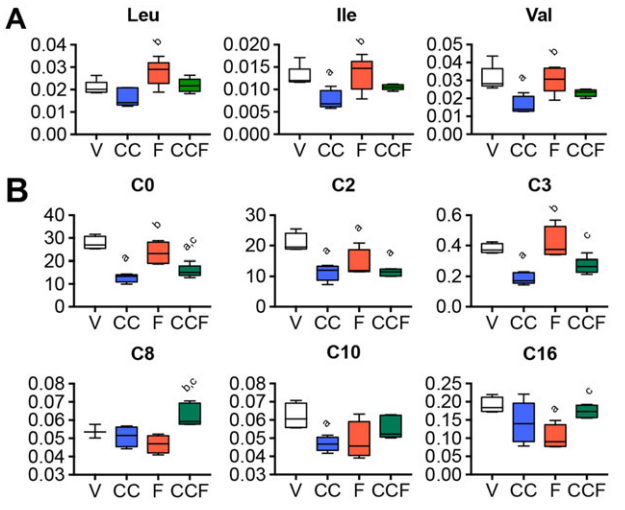


**Figure 4** Lipoprotein levels in the plasma of animals bearing cancer or exposed to chemotherapy. Low-density lipoprotein-particle (LDL-P, A), short-dense low-density lipoprotein-particle (sdLDL-P, B), and high-density lipoprotein-particle (HDL-P, C) levels (expressed in mM) in the plasma of vehicle-treated animals (V), C26 hosts (CC), Folfiri-treated mice (F), or Folfiri-treated tumour bearers (CCF). Data are expressed as means ± standard deviation. Statistical significance was evaluated by two-way analysis of variance, and significant differences (at least $P < 0.05$) were reported as $^{a}P$ vs. V; $^{b}P$ vs. CC; $^{c}P$ vs. F.

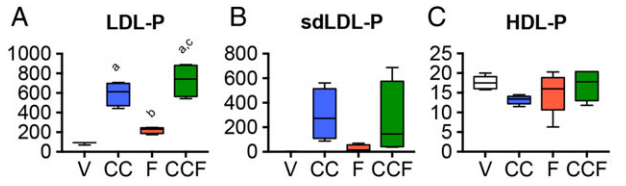


P particle numbers in the CC group were more than sevenfold higher than the V group. An increase of 2.6-fold was observed for the F group, although this difference did not reach significance. The effect appears to be additive yielding an increase of 8.6-fold in the CCF group. As shown in *Figure* 4B, the small-dense LDL-Ps appeared to be the major components of this increased LDL particle count. The HDL-P levels shown in *Figure* 4C showed a much less dramatic reduction in HDL-P in the CC group, although this was not significant.

In order to clarify whether there was altered uptake of LDL particles from the blood, LDL-receptor levels in muscle and liver were quantified (Supporting Information, *Figure* S1). Interestingly, the levels of the muscle LDL receptor were upregulated in all of the experimental groups with larger increases in the CC and CCF groups (Supporting Information, *Figure* S1A), while no significant change was observed in the liver (Supporting Information, *Figure* S1B). This indicates that the observed effects are not simply due to decreased uptake in the muscle.

## *Increased inflammation in cancer cachexia*

Another blood-based biomarker that was measured is an aggregate signal of *N*-acetyl glycan groups primarily attached to acute phase proteins called GlycA.[22] This biomarker has been associated with various inflammatory conditions including arthritis, coronary heart disease, and colorectal cancer. In our study, the levels of GlycA were significantly increased by around 30% in the CC and CCF groups but not in the F group (*Figure* 5A). This is consistent with an expected inflammatory state with cancer cachexia and a lack of inflammation with chemotherapy.


DOI: 10.1002/jcsm.12360

**Figure 5** Circulating glycoprotein acetylation (GlycA) and muscle reactive oxygen species (ROS) levels. Circulating GlycA marker levels (expressed in mM) (A) and ROS levels (expressed in arbitrary units, AU) (B) in the skeletal muscle of vehicle-treated animals (V), C26 hosts (CC), Folfiri-treated mice (F), or Folfiri-treated tumour bearers (CCF). Data are expressed as means ± standard deviation. Statistical significance was evaluated by two-way analysis of variance, and significant differences (at least $P < 0.05$) were reported as $^{a}P$ vs. V; $^{b}P$ vs. CC; $^{c}P$ vs. F.

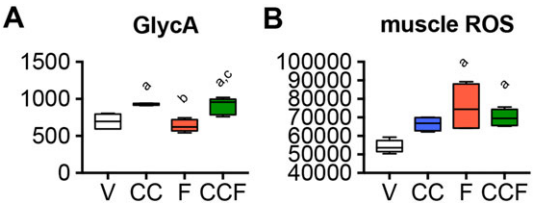


## *Cancer cachexia and chemotherapy both lead to increased skeletal muscle reactive oxygen species*

Oxidative stress is thought to play a role in both cancer cachexia and some of the adverse effects of chemotherapy. In order to evaluate this, we used 2′,7′-dichlorofluorescin diacetate as a probe to measure the ROS in skeletal muscle. *Figure* 5B shows that the ROS levels in the F and CCF groups were significantly increased and the level trended higher with a *P*-value of 0.06 for the CC group. These data are consistent with previously published evidence.[6]

## *Muscle metabolome shows overall decline in energy metabolism*

The next step in the investigation was to understand the metabolic effects in the skeletal muscle by examining the metabolic profiles of quadriceps muscle in mice bearing cancer or exposed to chemotherapy. *Figure* 6 shows the levels of several metabolites from the glycolysis and TCA cycle pathways. A composite measurement of glycogen in the muscle suggested no significant differences in the carbohydrate demands in the experimental groups. To further evaluate any potential alterations in glycolysis in muscle, we measured the enzymatic activity of hexokinase, the first step in the glycolytic pathway (*Figure* 7A). The activity levels were consistent with V in the CC and F groups but significantly reduced in the CCF group.

The consistent levels of lactate across all groups suggest pyruvate is still entering into the TCA cycle in the muscle. In order to evaluate the entry of pyruvate into the TCA cycle,

**Figure 6** Muscle glycolysis and tricarboxylic acid (TCA) cycle intermediates are affected by cancer and chemotherapy. Representative diagram of glycolysis and TCA cycle showing the metabolite concentration (expressed in mM) detected in the skeletal muscle of vehicle-treated animals (V), C26 hosts (CC), Folfiri-treated mice (F), or Folfiri-treated tumour bearers (CCF). Data are expressed as means ± standard deviation. Statistical significance was evaluated by two-way analysis of variance, and significant differences (at least $P < 0.05$) were reported as $^{a}P$ vs. V; $^{b}P$ vs. CC; $^{c}P$ vs. F.

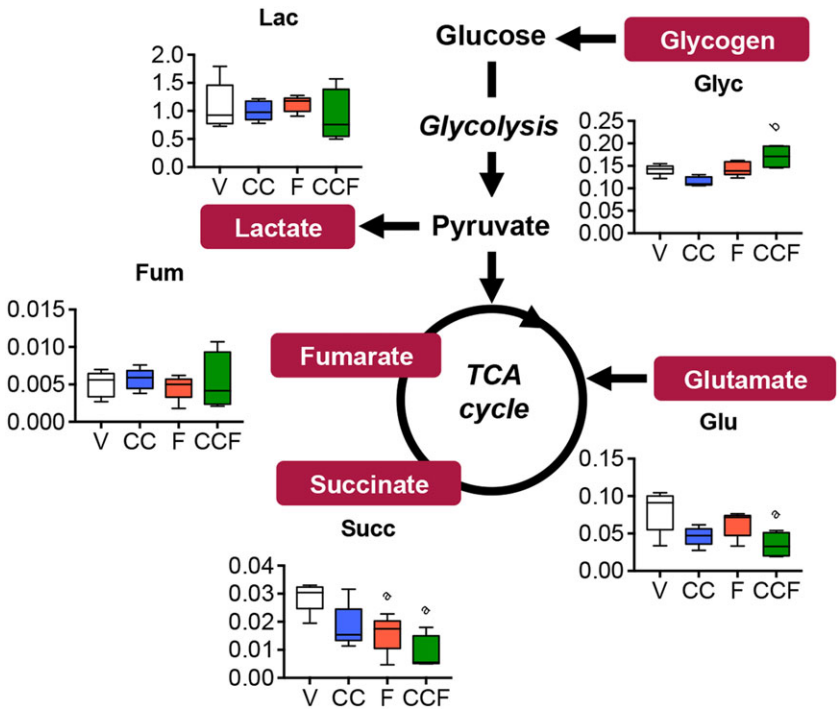



DOI: 10.1002/jcsm.12360

**Figure 7** Muscle enzymatic activities. The enzymatic activities of hexokinase (HK, A), pyruvate dehydrogenase (PDH, B), citrate synthase (CS, C), and succinate dehydrogenase (SDH, D) in the skeletal muscle of vehicle-treated animals (V), C26 hosts (CC), Folfiri-treated mice (F), or Folfiri-treated tumour bearers (CCF) were expressed in milliunits/mL (mU/mL). Data are expressed as means ± standard deviation. Statistical significance was evaluated by two-way analysis of variance, and significant differences (at least $P < 0.05$) were reported as $^{a}P$ vs. V; $^{b}P$ vs. CC; $^{c}P$ vs. F.

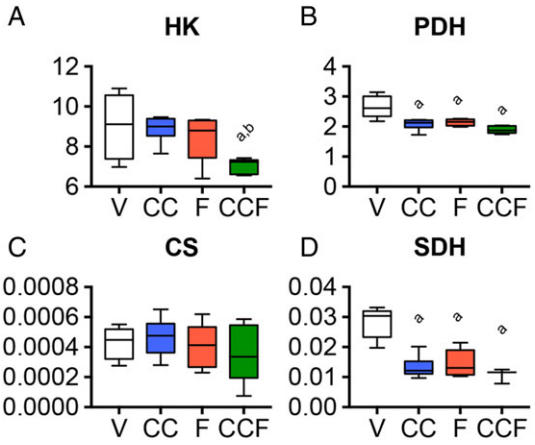


**Figure 8** Muscle metabolites involved in amino acid and fatty acid metabolism. Leucine (Leu), isoleucine (Ile), and valine (Val) levels (expressed in mM) in the skeletal muscle of vehicle-treated animals (V), C26 hosts (CC), Folfiri-treated mice (F), or Folfiri-treated tumour bearers (CCF) (A). Free carnitine (C0), acetylcarnitine (C2), acylcarnitine (C3), octanoylcarnitine (C8), decanoylcarnitine (10), and palmitoylcarnitine (16) levels (expressed in mM) in the muscle of vehicle-treated animals (V), C26 hosts (CC), Folfiri-treated mice (F), or Folfiri-treated tumour bearers (CCF) (B). Data are expressed as means ± standard deviation. Statistical significance was evaluated by two-way analysis of variance, and significant differences (at least $P < 0.05$) were reported as $^{a}P$ vs. V; $^{b}P$ vs. CC; $^{c}P$ vs. F.

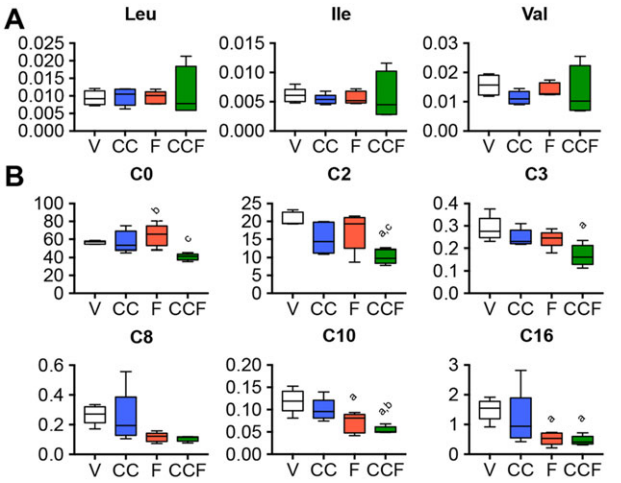


we measured the activity of the enzyme PDH. This enzyme catalyses the transformation of pyruvate into acetyl-CoA. As shown in *Figure* 7B, the activity of PDH in each of the experimental groups was reduced by between 20 and 30% indicating reduced flux of glycolysis-derived pyruvate into the TCA cycle.

A combination of enzymatic activity and metabolite measurements were conducted to evaluate the flux through the TCA cycle. Despite the reduced entry of pyruvate into the TCA cycle, the enzymatic activities for the next two steps in the TCA cycle were not significantly altered (*Figure* 7C). Citrate synthase transforms oxaloacetate and acetyl-CoA into citrate. Glutamate is an anapleurotic substrate for the TCA cycle; that is, it can enter the cycle to replenish any metabolites that may be lost due from biosynthetic processes. Although not statistically significant, the trend of reduced glutamate in the experimental groups is also consistent with a reduced TCA cycle flux. The reduced levels of succinate, particularly in F and CCF, were consistent with decreased flux through the TCA cycle. Similarly, the enzymatic activity of SDH for each of the groups (*Figure* 7D) further supports reduced TCA cycle flux in the experimental groups. Given that SDH is also a component of the electron transport chain, this could also indicate a decrease in oxidative phosphorylation.

Metabolic profiles from the BCAAs and fatty acid oxidation pathways in the muscle are shown in *Figure* 8. Unlike in plasma, the BCAA levels in muscle appear consistent across the groups (*Figure* 8A). *Figure* 8B shows that the free carnitine (C0) levels were also consistent, suggesting no major differences in fatty acid entry into the mitochondria. A trend of reduced acetylcarnitine (C2) levels was observed in the CC group (*P*-value = 0.13), and a significant decrease was observed in the CCF group suggesting an overall reduction in acetyl-CoA production. The C3 AC levels suggested a reduced flux through β-oxidation with the effect being significant in the CCF group. No significant differences in the long and medium chain ACs were observed for the CC group, but significant reductions in C10 and C16 species were observed in both the F and CCF groups. This suggested that chemotherapy induces a more pronounced reduction in β-oxidation than cancer cachexia.

The levels of three major energy-related metabolites were measured in the muscle tissue and were consistent with reduced energy production (*Figure* 9). A significant reduction in adenosine triphosphate (ATP) was observed in each of the experimental groups, along with a consistent increase in adenosine monophosphate (AMP) levels in the F group only. Another energy carrier, creatine phosphate, was lower in each of the experimental groups, consistent with reduced cellular energy production.


DOI: 10.1002/jcsm.12360

**Figure 9** Muscle energy metabolites. Adenosine triphosphate (ATP), adenosine monophosphate (AMP), and creatine phosphate (CrtnP) levels (expressed in mM) in the muscle of vehicle-treated animals (V), C26 hosts (CC), Folfiri-treated mice (F), or Folfiri-treated tumour bearers (CCF). Data are expressed as means ± standard deviation. Statistical significance was evaluated by two-way analysis of variance, and significant differences (at least $P < 0.05$) were reported as $^{a}P$ vs. V; $^{b}P$ vs. CC; $^{c}P$ vs. F.

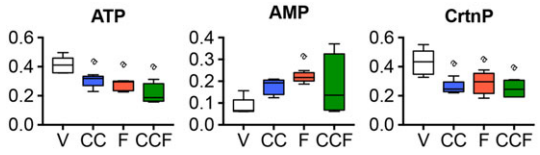


## *Liver metabolome suggests increased gluconeogenesis and tricarboxylic acid cycle flux with chemotherapy*

A significant depletion in both liver glucose and glycogen in each of the experimental groups, shown in *Figure* 10, was consistent with an increased systemic demand for glucose. A major function of the liver is to use non-carbohydrate sources to generate additional glucose under conditions of high glucose demand as would be expected with a malignancy. The gluconeogenic process can use lactate and alanine as precursors. The lactate levels were not significantly altered in the experimental groups, but there was a trend towards

**Figure 10** Liver glycolysis/gluconeogenesis and tricarboxylic acid (TCA) cycle intermediates are affected by cancer and chemotherapy. Representative diagram of glycolysis and TCA cycle showing the metabolite concentration (expressed in mM) detected in the liver of vehicle-treated animals (V), C26 hosts (CC), Folfiri-treated mice (F), or Folfiri-treated tumour bearers (CCF). Data are expressed as means ± standard deviation. Statistical significance was evaluated by two-way analysis of variance, and significant differences (at least $P < 0.05$) were reported as $^{a}P$ vs. V; $^{b}P$ vs. CC; $^{c}P$ vs. F.

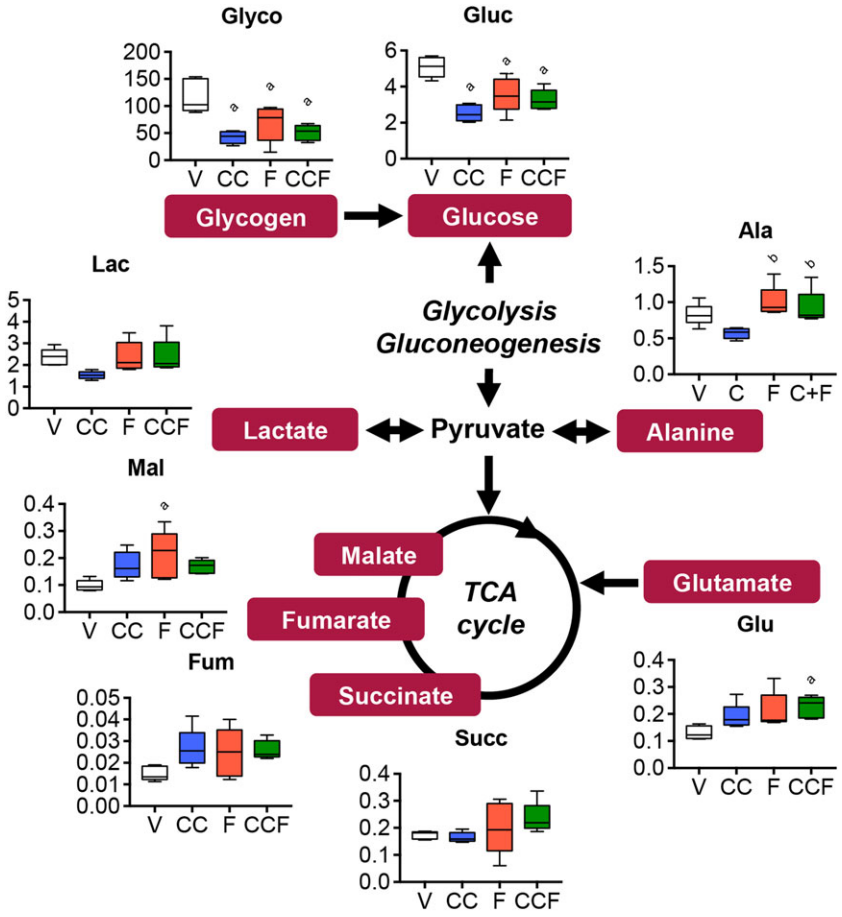



DOI: 10.1002/jcsm.12360

lower values in the CC group. For alanine, the trend for lower levels in the CC group remained, but the trend was reversed for the F and CCF groups.

In the TCA cycle, the levels of fumarate and malate appeared to trend higher levels in the experimental groups, but only the level of malate in the F group met statistical significance. The anapleurotic substrate glutamate also showed higher levels in the experimental groups with the levels in the F and CCF groups meeting statistical significance. In contrast to the muscle, it appears that TCA cycle activity was increased in the liver.

To further interrogate the gluconeogenic process, we measured the gene expression levels of PEPCK, a critical enzyme that is activated in gluconeogenesis. Interestingly, a significant increase in liver PEPCK was only observed for the F group (Supporting Information, *Figure* S2).

## Discussion

The goal of this study was to provide a comprehensive metabolomics investigation of the differences between cancer-induced and chemotherapy-induced cachexia. Given that cachexia is a severe form of energy imbalance, we focused our analytical approaches on the major cellular energetic pathways. By analysing samples from plasma, muscle, and liver, we were able to construct a more holistic picture of the energetic derangements that are associated with these different types of cachexia.

Our results indicate that systemic glucose metabolism is clearly impacted in both cancer-induced and chemotherapy-induced cachexia. Circulating glucose levels were reduced in all experimental groups. One possible factor contributing to the hypoglycaemia is reduced food intake. Although food intake was not monitored in our study, in a recent study aimed at characterizing the functional and metabolic impairments associated with the C26 cachexia model, Murphy *et al*. showed that control mice, pair fed to severely cachectic C26 tumour-bearing mice, had no significant difference in muscle mass compared with *ad libitum* fed control mice, despite significantly reduced food intake. This suggests that the changes observed in the cancer hosts were primarily linked to the growth of the C26 tumour.[24] A recent study from our laboratory showed only transient drops in food intake after initiation of Folfiri treatment, but no significant differences in the average food consumption were observed over the entire experimental period.[6] Although we cannot rule out a reduced food intake leading to the hypoglycaemia in the CC group, we do not expect this to be a factor in the F group. Additionally, the consistently reduced levels of liver glycogen in all three groups support a state of increased glucose demand in cachexia from both cancer and chemotherapy.

In a previous study from our laboratory comparing C26 tumour-bearing mice with mice on a calorie-restricted diet equivalent to a 40% reduction in caloric intake, we found a significant increase in the concentration of serum, β-hydroxybutyrate, a metabolite that would be expected to increase under starvation conditions.[25] No significant differences in the levels of serum β-hydroxybutyrate across any of the three groups were observed suggesting that the metabolic phenotype was not due to a dramatic reduction in caloric intake.

Increased expression of the PEPCK gene in both groups is consistent with an up-regulation of gluconeogenesis to accommodate the increased systemic demand. In the case of the CC group, it is reasonable to postulate that much of the glucose is being consumed by the tumour. The source of the increased glucose demand is not as clear in the F and CCF groups, where the effect does not seem to be driven by muscle metabolism. The stable levels of muscle glycogen in the experimental groups suggest that glucose demand is not significantly altered. The steady lactate levels also indicate that the muscles have not switched to a predominantly glycolytic metabolism.

Analysis of the TCA cycle indicates some significant differences associated with cancer-induced and chemotherapy-induced cachexia. Very significant reductions in the plasma levels of citrate and succinate were observed in the CC group, while no significant changes were found in the F group. These differences between groups are not found in the muscle tissue with both the CC and F groups showing reduced flux through the TCA cycle as indicated by reduced activity of PDH and SDH along with reduced levels of succinate. A reduction in PDH activity is expected under conditions of metabolic stress, including nutrient deprivation and hypoxia wherein PDH is inactivated by PDH kinases.[26,27] The exact nature of the metabolic stresses imposed by malignancy and chemotherapy may be different, but they both lead to similar inactivation of PDH.

A number of studies have indicated that the activity of the TCA cycle is reduced in cachexia. A mass spectrometry-based flux analysis found that the TCA cycle flux in muscle was significantly reduced in a Lewis lung carcinoma model of cancer cachexia.[28] A recent proteomics study of muscle tissue from our lab identified reduced expression of proteins related to oxidative phosphorylation, TCA cycle, and glycolysis in both C26 hosts and Folfiri-treated mice,[5] thus suggesting that alterations of mitochondrial function may play a relevant role in causing muscle wasting in these conditions. This was also consistent with our previous reports, showing that mitochondrial abnormalities generally occur following cancer growth[4] or chemotherapy treatment.[6]

Interestingly, the liver showed the opposite effect with a trend towards increased levels of the TCA cycle intermediates, fumarate, and malate along with the anapleurotic amino acid glutamate. This increase in oxidative metabolism


DOI: 10.1002/jcsm.12360

could be required to provide energy for the increase in gluconeogenesis and, in the case of the cancer cachexia group, an increased production of acute phase proteins, in line with our previous observations.[19]

Significant reduction in the plasma levels of free amino acids, in particular the BCAAs, has been observed in patients with cachexia.[15,25,29] In addition to providing building blocks for protein synthesis, BCAAs also play a role in signal transduction pathways that modulate protein synthesis.[30] Under conditions of starvation, the circulating levels of BCAAs have been shown to increase along with a significant decrease in BCAA oxidation.[31] Enhanced rates of BCAA oxidation have been observed in whole body and skeletal muscle during sepsis, trauma, and after endotoxin or tumour necrosis factor treatment.[32–34] It should be noted that each of these conditions is associated with cachexia. Interestingly, the F group had little change in circulating BCAA levels, but some of that may be due to the smaller extent of weight loss in that group. The CCF group had very similar overall loss in body weight but even more weight loss in gastrocnemius, tibialis, and quadriceps than the CC group. The BCAA levels in the F group are all significantly higher than the CC group, which may indicate that Folfiri treatment confers a more starvation-like phenotype where more BCAAs are released into the circulation before oxidation. This would suggest that the cachexia induced by Folfiri may not be effectively treated with supplemental amino acids or related metabolites.

In our study, the levels of BCAAs in the skeletal muscle were rather stable across the four groups. This somewhat surprising result may be a function of the particular tissue that we analysed. The quadriceps is composed of predominantly type IIB muscle fibres, which are fast twitch fibres with low oxidative and high glycolytic activity. This lower dependence upon oxidative metabolism may be the cause of the more stable BCAA levels. Future studies should look at the metabolic profiles of other types of skeletal muscle.

A recent study of kidney cancer by Fukawa *et al*. found that excessive fatty acid oxidation was a major driver of muscle wasting in cancer cachexia and they suggest that mitigation of this excess may be a promising therapeutic approach.[17] By applying media from a highly cachexia-inducing cancer cell line onto C2C12 cells, this group found a dramatic increase in ACs indicative of increased fatty acid oxidation. They followed these results with an *in vivo* model, where they used etomoxir, a carnitine palmitoyl transferase 1 inhibitor to block fatty acid oxidation. They found significantly reduced levels of ACs along with a rescue of skeletal muscle mass. In contrast, our data suggest that fatty acid oxidation is reduced in both the CC and F groups but to different extents. It is interesting to note that the CC group displays significant hyperlipidaemia as evidenced by the dramatically elevated LDL particle numbers, while also having reduced levels of C0 indicating reduced ability of fatty acids to enter the β-oxidation pathway. The hyperlipidaemia in the F group is more moderate, and the C0 levels in this group are not significantly different from vehicle-treated controls. The increased levels of ACs found in the study by Fukawa *et al*.[17] indicate increased flux, but an increase in ACs can also be the result of incomplete fatty acid oxidation due to mitochondrial overload as demonstrated in the high-fat-diet model by Koves *et al*.[35] In our study, the reduced levels of ACs are consistent with reduced fatty acid oxidation, but given the potential for both cancer and chemotherapy to induce mitochondrial defects, the levels of ACs may also be influenced by these defects leading to build-up of certain ACs. The distinctly different AC profiles in the CC and F group compared with kidney cancer model reported by Fukawa *et al*.[17] indicate that targeting a reduction in fatty acid oxidation to combat these forms of cachexia is less promising.

Mitochondrial ATP synthesis has been shown to be severely impaired in skeletal muscle in cancer cachexia.[36] Our study shows reduced production of both muscle ATP and creatine phosphate in the CC and F groups. Cachectic muscle has been shown to have dysfunctions in the electron transport chain[37] and increased expression of mitochondrial uncoupling proteins (UCPs).[38–40] The UCPs promote proton leak across the inner mitochondrial membrane, reducing the proton gradient, generating heat, and reducing the production of ATP. Both cancer and chemotherapy have been associated with increases in oxidative stress, and in both cases, an up-regulation of UCPs may be a compensatory mechanism to inhibit oxidative phosphorylation, thereby reducing oxidative stress.[41,42] The decreased levels of ATP can also induce a signalling cascade that reduces protein synthesis. When the AMP/ATP ratio is high, the adenosine monophosphate-activated protein kinase (AMPK) is activated leading to downstream inhibition of mammalian target of rapamycin(mTOR)-mediated protein synthesis.

Intravenous injection of ATP has been used in a clinical trial on advanced non-small-cell lung cancer patients. In this study, the cachectic patients receiving ATP experienced no significant weight loss, whereas those not receiving ATP lost an average of 1.6 kg of body weight over a 1 month period.[43,44] Our results suggest that supplemental ATP may indeed provide some benefit with both cancer-induced and chemo-induced cachexia.

One of the most striking findings was the difference in the lipoprotein alterations between the CC and F groups. Hyperlipidaemia, including increased levels of circulating free fatty acids, triglycerides, and cholesterol, has been observed in cancer cachexia and an earlier metabolomics study on the C26 cachexia model reported elevations in VLDL and LDL levels.[15] An observation of increased LDL and decreased HDL similar to that found here was found in end-stage renal disease, and the proposed mechanism may shed some light on what is happening in cachexia.[45–47] Under normal


DOI: 10.1002/jcsm.12360

circumstances, intermediate density lipoproteins (IDLs) are converted to cholesterol ester-rich LDLs, which are cleared by the liver via the LDL receptor. The conversion of IDL to LDL involves the action of cholesterol ester transfer protein, which exchanges triglycerides from the IDL with cholesterol esters from HDL particles. End-stage renal disease is characterized by reduced levels of HDL and by hepatic lipase deficiency. These abnormalities lead to the accumulation of IDLs and formation of cholesterol-poor, triglyceride-rich, small-dense LDL particles. These particles have lower affinity for LDL receptor; thus, despite the lack of change in the liver LDL receptor and the increase in the muscle LDL receptor, these small-dense LDL particles may remain in circulation because of reduced binding affinity. This effect will be exacerbated by the continued reduction in skeletal muscle mass. Further studies will be conducted to see if these mechanisms are at play in cancer cachexia.

Our observation of oxidative stress in both cancer-induced and chemotherapy-induced cachexia is concordant with previous studies. Oxidative stress has been consistently observed in experimental models of cancer cachexia. Using the Yoshida AH-130 rat hepatoma model, Barreiro *et al*. found increased levels of malondialdehyde, a decomposition product of oxidized lipids, along with an associated up-regulation of the ubiquitin proteasome system.[48] Oxidative stress is also found with many chemotherapeutics. In fact, the primary mechanism of many chemotherapeutic drugs involves the formation of ROS to kill the tumour.[49] This can lead to an overall depletion of the endogenous antioxidant defence systems. In skeletal muscle, exposure to elevated antioxidants is known to cause muscle weakness and accelerate the rate of fatigue.[50,51] There is much debate on whether antioxidant supplementation can alter the efficacy of chemotherapeutics, but a systematic review found no evidence of antioxidant interference with chemotherapy mechanisms and a possibility that antioxidants may even improve tumour response and patient survival.[49] Antioxidant treatment may therefore be beneficial in both treating the tumour and sparing the skeletal muscle damage induced by the tumour, thereby enabling patients to complete their therapeutic regimen and thus improve survival.

The inflammatory marker GlycA presents a clear difference between the CC and F groups. This NMR-detectable plasma biomarker is an aggregate signal of acute phase glycoproteins and has been observed to be higher in patients with inflammatory conditions such as diabetes, rheumatoid arthritis,[52,53] cancer,[52,54,55] and insulin resistance.[56] It is well established that the growth of the C26 tumour leads to a significant increase in interleukin-6 (IL-6) levels, which correlate with the loss of body weight[57] and lead to hepatic synthesis and secretion of acute phase proteins.[58] In a recent study of rheumatoid arthritis, GlycA was significantly correlated with circulating IL-6.[59] Some chemotherapeutics, such as cyclophosphamide-doxorubicin-5-fluorouracil, can lead to increases in IL-6 production, thus promoting changes in body composition and fatigue.[60] However, in our previous studies conducted in Folfiri-treated mice, no STAT3 phosphorylation was observed, indicating that the STAT3/IL-6 pathway was not directly involved in the muscle wasting observed following Folfiri administration.[57] Thus, it appears that the lack of alteration of GlycA in the F group is likely due to an insignificant activation of the IL-6 pathway.

In cancer, the observation of systemic inflammation has been associated with an increase in ubiquitin proteasome mediated muscle wasting.[61] The observations of increases in the ubiquitin proteasome system with chemotherapy have been inconsistent,[6] further suggesting that, at least in the case of Folfiri, the inflammatory system is less involved.

This study revealed a number of critical differences in the metabolic effects of cancer-induced and chemotherapy-induced cachexia, but it is important to highlight the differences observed when chemotherapy is added to the cachexia model. Some of the observed changes in the CCF group are consistent with the changes observed in the other treatment groups. For example, the serum glucose levels as well as the liver glucose and glycogen levels are consistently reduced in all treatment groups. Many of the most significant metabolic effects observed in the CCF group are close to the CC group such as serum citrate, succinate, and short chain ACs, GlycA, and LDL-P. These similarities may be due to the higher levels of weight loss in these two groups. There are only few observations of metabolites where the CCF levels are closer to the F group than the CC group. These include serum lactate, muscle glycogen, and liver alanine. In each of these examples, the CCF levels are, in fact, not different from the V group. These observations, although subtle, demonstrate that some chemotherapy-induced perturbations may be greater than the cancer-induced perturbations.

## Conclusions

The results of this comprehensive metabolic profiling demonstrate that cancer-induced and chemotherapy-induced cachexia is characterized by a number of common and unique metabolic derangements. Both treatments led to an up-regulated systemic glucose demand, with decreased circulating glucose, and significant depletion of liver glucose and glycogen. Significant differences between cancer and chemotherapy were observed in amino acid catabolism and flux through the TCA cycle and β-oxidation pathways. Distinct differences were also observed in lipoprotein metabolism and inflammation. The results of this study make it clear that therapeutic interventions for cachexia must take into account the specific pathological or pharmacological driver of the cachexia. Given the heterogeneity of cachectic phenotypes


DOI: 10.1002/jcsm.12360

induced by cancer and chemotherapy, it must be recognized that the results of this study may be unique to the specific models used. New studies are underway with additional cancer-induced and chemotherapy-induced models of cachexia to further explore the common and unique metabolic drivers of cachexia.

## Author contributions

F.P., A.B., and T.M.O. conceived and designed the experiments; F.P., R.B., and A.B. performed the *in vivo* experiments, the body composition assessment, the muscle function analysis, and the molecular characterization of cachexia; F.P. and T.M.O. analysed the metabolomics data; F.P., M.E.C., A.B., and T.M.O. wrote and edited the paper.

## Acknowledgements

The authors certify that they comply with the ethical guidelines for authorship and publishing of the *Journal of Cachexia, Sarcopenia and Muscle*.[62] The authors would like to thank the staff at the Metabolomics Laboratory at the David H. Murdock Research Institute for metabolomics data collection. The authors would like to thank Teresa A. Zimmers, PhD, for sharing lab equipment and instruments for the characterization of cachexia in experimental animals. This study was supported by the Department of Surgery and the Department of Otolaryngology–Head & Neck Surgery at Indiana University and by grants from the V Foundation for Cancer Research (V2017-021 to A.B.), the American Cancer Society (Research Scholar Grant 132013-RSG-18-010-01-CCG to A.B.) and the IUSCC (IUSCC Associate Member Pilot Funding Mechanism to A.B. and T.M.O.).

## Online supplementary material

Additional supporting information may be found online in the Supporting Information section at the end of the article.

**Figure S1.** Supporting info item
**Figure S2.** Supporting info item

## Conflict of interest

The authors declare no conflict of interest.

## References

1. Fearon K, Strasser F, Anker SD, Bosaeus I, Bruera E, Fainsinger RL, et al. Definition and classification of cancer cachexia: an international consensus. *Lancet Oncol* 2011;**12**:489–495.
2. Tisdale MJ. Cachexia in cancer patients. *Nat Rev Cancer* 2002;**2**:862–871.
3. Evans WJ, Morley JE, Argiles J, Bales C, Baracos V, Guttridge D, et al. Cachexia: a new definition. *Clin Nutr* 2008;**27**:793–799.
4. Pin F, Busquets S, Toledo M, Camperi A, Lopez-Soriano FJ, Costelli P, et al. Combination of exercise training and erythropoietin prevents cancer-induced muscle alterations. *Oncotarget* 2015;**6**:43202–43215.
5. Barreto R, Mandili G, Witzmann FA, Novelli F, Zimmers TA, Bonetto A. Cancer and chemotherapy contribute to muscle loss by activating common signaling pathways. *Front Physiol.* 2016;**7**:472.
6. Barreto R, Waning DL, Gao H, Liu Y, Zimmers TA, Bonetto A. Chemotherapy-related cachexia is associated with mitochondrial depletion and the activation of ERK1/2 and p38 MAPKs. *Oncotarget.* 2016;**7**:43442–43460.
7. Argiles JM, Lopez-Soriano FJ, Busquets S. Muscle wasting in cancer: the role of mitochondria. *Curr Opin Clin Nutr Metab Care* 2015;**18**:221–225.
8. de Vos-Geelen J, Fearon KC, Schols AM. The energy balance in cancer cachexia revisited. *Curr Opin Clin Nutr Metab Care* 2014;**17**:509–514.
9. Le Bricon T, Gugins S, Cynober L, Baracos VE. Negative impact of cancer chemotherapy on protein metabolism in healthy and tumor-bearing rats. *Metabolism: clinical and experimental* 1995;**44**:1340–1348.
10. Damrauer JS, Stadler ME, Acharyya S, Baldwin AS, Couch ME, Guttridge DC. Chemotherapy-induced muscle wasting: association with NF-κB and cancer cachexia. *Basic Applied Myology* 2008;**18**:139–148.
11. Chen JA, Splenser A, Guillory B, Luo J, Mendiratta M, Belinova B, et al. Ghrelin prevents tumour- and cisplatin-induced muscle wasting: characterization of multiple mechanisms involved. *J Cachexia Sarcopenia Muscle* 2015;**6**:132–143.
12. Garcia JM, Scherer T, Chen JA, Guillory B, Nassif A, Papusha V, et al. Inhibition of cisplatin-induced lipid catabolism and weight loss by ghrelin in male mice. *Endocrinology* 2013;**154**:3118–3129.
13. Gilliam LA, St Clair DK. Chemotherapy-induced weakness and fatigue in skeletal muscle: the role of oxidative stress. *Antioxid Redox Signal* 2011;**15**:2543–2563.
14. ultani M, Stringer AM, Bowen JM, Gibson RJ. Anti-inflammatory cytokines: important immunoregulatory factors contributing to chemotherapy-induced gastrointestinal mucositis. *Chemother Res Pract* 2012;**2012**:490804.
15. O'Connell TM, Ardeshirpour F, Asher SA, Winnike JH, Yin X, George J, et al. Metabolomic analysis of cancer cachexia reveals distinct lipid and glucose alterations. *Metabolomics* 2008;**4**:216–225.
16. Der-Torossian H, Wysong A, Shadfar S, Willis MS, McDunn J, Couch ME. Metabolic derangements in the gastrocnemius and the effect of compound A therapy in a murine model of cancer cachexia. *J Cachexia Sarcopenia Muscle* 2013;**4**:145–155.
17. Fukawa T, Yan-Jiang BC, Min-Wen JC, Jun-Hao ET, Huang D, Qian CN, et al. Excessive fatty acid oxidation induces muscle atrophy in cancer cachexia. *Nat Med* 2016;**22**:666–671.
18. Bonetto A, Rupert JE, Barreto R, Zimmers TA. The Colon-26 carcinoma tumor-bearing mouse as a model for the study of cancer cachexia. *Journal of visualized experiments: JoVE* 2016;**117**.
19. Bonetto A, Aydogdu T, Kunzevitzky N, Guttridge DC, Khuri S, Koniaris LG, et al. STAT3 activation in skeletal muscle links muscle wasting and the acute phase response in cancer cachexia. *PloS one.* 2011;**6**:e22538.
20. Bonetto A, Andersson DC, Waning DL. Assessment of muscle mass and strength in mice. *Bonekey Rep* 2015;**4**:732.

21. Beckonert O, Keun HC, Ebbels TM, Bundy J, Holmes E, Lindon JC, Nicholson JK. Metabolic profiling, metabolomic and metabonomic procedures for NMR spectroscopy of urine, plasma, serum and tissue extracts. *Nat Protoc.* 2007;**2**(11):2692–703.
22. Jeyarajah EJ, Cromwell WC, Otvos JD. Lipoprotein particle analysis by nuclear magnetic resonance spectroscopy. *Clin Lab Med* 2006;**26**:847–870.
23. Otvos JD, Shalaurova I, Wolak-Dinsmore J, Connelly MA, Mackey RH, Stein JH, et al. GlycA: a composite nuclear magnetic resonance biomarker of systemic inflammation. *Clin Chem* 2015;**61**:714–723.
24. Murphy KT, Chee A, Trieu J, Naim T, Lynch GS. Importance of functional and metabolic impairments in the characterization of the C-26 murine model of cancer cachexia. *Dis Model Mech* 2012;**5**:533–545.
25. Der-Torossian H, Asher SA, Winnike JH, Wysong A, Yin X, Willis MS, et al. Cancer cachexia's metabolic signature in a murine model confirms a distinct entity. *Metabolomics.* 2013;**9**:730–739.
26. Kim JW, Tchernyshyov I, Semenza GL, Dang CV. HIF-1-mediated expression of pyruvate dehydrogenase kinase: a metabolic switch required for cellular adaptation to hypoxia. *Cell Metab* 2006;**3**:177–185.
27. Spriet LL, Tunstall RJ, Watt MJ, Mehan KA, Hargreaves M, Cameron-Smith D. Pyruvate dehydrogenase activation and kinase expression in human skeletal muscle during fasting. *J Appl Physiol* (1985) 2004;**96**(6):2082–2087.
28. Tzika AA, Fontes-Oliveira CC, Shestov AA, Constantinou C, Psychogios N, Righi V, et al. Skeletal muscle mitochondrial uncoupling in a murine cancer cachexia model. *Int J Oncol* 2013;**43**:886–894.
29. Beck SA, Tisdale MJ. Nitrogen excretion in cancer cachexia and its modification by a high fat diet in mice. *Cancer Res* 1989;**49**:3800–3804.
30. Yoshizawa F. Regulation of protein synthesis by branched-chain amino acids *in vivo*. *Biochem Biophys Res Commun* 2004;**313**: 417–422.
31. Holecek M, Sprongl L, Tilser I. Metabolism of branched-chain amino acids in starved rats: the role of hepatic tissue. *Physiol Res* 2001;**50**:25–33.
32. Holecek M. Leucine metabolism in fasted and tumor necrosis factor-treated rats. *Clin Nutr* 1996;**15**:91–93.
33. Holecek M, Tilser I, Skopec F, Sprongl L. Leucine metabolism in partially hepatectomized rats. *J Hepatol* 1997;**26**:1141–1147.
34. Nawabi MD, Block KP, Chakrabarti MC, Buse MG. Administration of endotoxin, tumor necrosis factor, or interleukin 1 to rats activates skeletal muscle branched-chain alpha-keto acid dehydrogenase. *J Clin Invest* 1990;**85**:256–263.
35. Koves TR, Ussher JR, Noland RC, Slentz D, Mosedale M, Ilkayeva O, et al. Mitochondrial overload and incomplete fatty acid oxidation contribute to skeletal muscle insulin resistance. *Cell Metab* 2008;**7**:45–56.
36. Constantinou C, Fontes de Oliveira CC, Mintzopoulos D, Busquets S, He J, Kesarwani M, et al. Nuclear magnetic resonance in conjunction with functional genomics suggests mitochondrial dysfunction in a murine model of cancer cachexia. *Int J Mol Med* 2011;**27**:15–24.
37. McLean JB, Moylan JS, Andrade FH. Mitochondria dysfunction in lung cancer-induced muscle wasting in C2C12 myotubes. *Front Physiol* 2014;**5**:503.
38. Bing C, Russell ST, Beckett EE, Collins P, Taylor S, Barraclough R, et al. Expression of uncoupling proteins-1, -2 and -3 mRNA is induced by an adenocarcinoma-derived lipid-mobilizing factor. *Br J Cancer* 2002;**86**:612–618.
39. Collins P, Bing C, McCulloch P, Williams G. Muscle UCP-3 mRNA levels are elevated in weight loss associated with gastrointestinal adenocarcinoma in humans. *Br J Cancer* 2002;**86**:372–375.
40. Sanchis D, Busquets S, Alvarez B, Ricquier D, Lopez-Soriano FJ, Argiles JM. Skeletal muscle UCP2 and UCP3 gene expression in a rat cancer cachexia model. *FEBS Lett* 1998;**436**:415–418.
41. Divakaruni AS, Brand MD. The regulation and physiology of mitochondrial proton leak. *Physiology (Bethesda)* 2011;**26**:192–205.
42. Nedergaard J, Ricquier D, Kozak LP. Uncoupling proteins: current status and therapeutic prospects. *EMBO Rep* 2005;**6**:917–921.
43. Agteresch HJ, Dagnelie PC, van der Gaast A, Stijnen T, Wilson JH. Randomized clinical trial of adenosine 5′-triphosphate in patients with advanced non-small-cell lung cancer. *J Natl Cancer Inst* 2000;**92**:321–328.
44. Agteresch HJ, Rietveld T, Kerkhofs LG, van den Berg JW, Wilson JH, Dagnelie PC. Beneficial effects of adenosine triphosphate on nutritional status in advanced lung cancer patients: a randomized clinical trial. *J Clin Oncol* 2002;**20**:371–378.
45. Klin M, Smogorzewski M, Ni Z, Zhang G, Massry SG. Abnormalities in hepatic lipase in chronic renal failure: role of excess parathyroid hormone. *J Clin Invest* 1996;**97**: 2167–2173.
46. Liang K, Vaziri ND. Down-regulation of hepatic lipase expression in experimental nephrotic syndrome. *Kidney Int* 1997;**51**:1933–1937.
47. Sato T, Liang K, Vaziri ND. Protein restriction and AST-120 improve lipoprotein lipase and VLDL receptor in focal glomerulosclerosis. *Kidney Int* 2003;**64**:1780–1786.
48. Barreiro E, de la Puente B, Busquets S, Lopez-Soriano FJ, Gea J, Argiles JM. Both oxidative and nitrosative stress are associated with muscle wasting in tumour-bearing rats. *FEBS Lett* 2005;**579**:1646–1652.
49. Block KI, Koch AC, Mead MN, Tothy PK, Newman RA, Gyllenhaal C. Impact of antioxidant supplementation on chemotherapeutic toxicity: a systematic review of the evidence from randomized controlled trials. *Int J Cancer* 2008;**123**:1227–1239.
50. Powers SK, Jackson MJ. Exercise-induced oxidative stress: cellular mechanisms and impact on muscle force production. *Physiol Rev* 2008;**88**:1243–1276.
51. Supinski GS, Callahan LA. Free radical-mediated skeletal muscle dysfunction in inflammatory conditions. *J Appl Physiol* 2007;**102**:2056–2063.
52. Bell JD, Brown JC, Nicholson JK, Sadler PJ. Assignment of resonances for 'acute-phase' glycoproteins in high resolution proton NMR spectra of human blood plasma. *FEBS Lett* 1987;**215**:311–315.
53. Lauridsen MB, Bliddal H, Christensen R, Danneskiold-Samsoe B, Bennett R, Keun H, et al. 1H NMR spectroscopy-based interventional metabolic phenotyping: a cohort study of rheumatoid arthritis patients. *J Proteome Res* 2010;**9**:4545–4553.
54. Kriat M, Vion-Dury J, Fayre R, Maraninchi D, Harle JR, Confort-Gouny S, et al. Variations of plasma sialic acid and *N*-acetylglucosamine levels in cancer, inflammatory diseases and bone marrow transplantation: a proton NMR spectroscopy study. *Biochimie* 1991;**73**:99–104.
55. Chandler PD, Akinkuolie AO, Tobias DK, Lawler PR, Li C, Moorthy MV, et al. Association of N-linked glycoprotein acetyls and colorectal cancer incidence and mortality. *PloS one* 2016;**11**:e0165615.
56. Wurtz P, Makinen VP, Soininen P, Kangas AJ, Tukiainen T, Kettunen J, et al. Metabolic signatures of insulin resistance in 7,098 young adults. *Diabetes* 2012;**61**:1372–1380.
57. Bonetto A, Aydogdu T, Jin X, Zhang Z, Zhan R, Puzis L, et al. JAK/STAT3 pathway inhibition blocks skeletal muscle wasting downstream of IL-6 and in experimental cancer cachexia. *Am J Physiol Endocrinol Metab* 2012;**303**:E410–E421.
58. Dijk W, Turner GA, Mackiewicz A. Changes in glycosylation of acute-phase proteins in health and disease: occurence, regulation and function. *Glycoconj J* 1994;**1**:5–14.
59. Bartlett DB, Connelly MA, AbouAssi H, Bateman LA, Tune KN, Huebner JL, et al. A novel inflammatory biomarker, GlycA, associates with disease activity in rheumatoid arthritis and cardio-metabolic risk in BMI-matched controls. *Arthritis Res Ther* 2016;**18**:86.
60. Elsea CR, Kneiss JA, Wood LJ. Induction of IL-6 by cytotoxic chemotherapy is associated with loss of lean body and fat mass in tumor-free female mice. *Biol Res Nurs* 2015;**17**:549–557.
61. DeJong CH, Busquets S, Moses AG, Schrauwen P, Ross JA, Argiles JM, et al. Systemic inflammation correlates with increased expression of skeletal muscle ubiquitin but not uncoupling proteins in cancer cachexia. *Oncol Rep* 2005;**14**:257–263.
62. von Haehling S, Morley JE, Coats AJS, Anker SD. Ethical guidelines for publishing in the Journal of Cachexia, Sarcopenia and Muscle: update 2017. *J Cachexia Sarcopenia Muscle* 2017;**8**:1081–1083.